Estuaries Vol. 27, No. 3, p. 515–526 June 2004

Use of a Particle-tracking Model for Predicting Entrainment at Power Plants on the Hudson River

ALAN F. BLUMBERG[1,2,*], DENNIS J. DUNNING[3], HONGHAI LI[2], DOUGLAS HEIMBUCH[4], and W. ROCKWELL GEYER[5]

[1] *Stevens Institute of Technology, Department of Civil, Environmental and Ocean Engineering, Hoboken, New Jersey 07030*
[2] *HydroQual, Inc., 1200 MacArthur Boulevard, Mahwah, New Jersey 07430*
[3] *New York Power Authority, 123 Main Street, White Plains, New York 10601*
[4] *Allee, King, Rosen & Fleming, Inc., 7250 Parkway Drive, Suite 210, Hanover, Maryland 21076*
[5] *Department of Applied Ocean Physics and Engineering, Woods Hole Oceanographic Institution, Woods Hole, Massachusetts 02543*

ABSTRACT: A major assumption of the Empirical Transport Model (ETM), widely adopted by both electric utilities and regulatory agencies for estimating the effects of entrainment mortality on fish populations in estuaries, is that the fraction of ichthyoplankton entrained varies only in response to changes in water withdrawals, not to changes in freshwater flow. We evaluated this assumption using a particle-tracking model to estimate the probability of entrainment at power plants on the Hudson River during low and high freshwater flow periods and comparing those probabilities with estimates calculated from the ETM. We found that freshwater flow had a profound effect on the probability of entrainment. Both the number of river regions from which particles were entrained and the probabilities of entrainment for particles in those river regions differed between low-flow and high-flow periods. During high flow, particles spent less time in the grid box next to the intakes, reducing the probability of entrainment for particles released in the river region of each power plant and the average probability of entrainment across all regions at three power plants. The reduced probability of entrainment for particles released in the river regions of two power plants was offset by higher entrainment for particles upriver of these power plants. Although the average probabilities of entrainment across all river regions estimated with the particle-tracking model and the ETM were relatively similar for some power plants at high flow, low flow, or both, the probabilities for each river region differed considerably between the models. The number of river regions from which particles were entrained using the ETM was consistently underestimated, resulting in probabilities for regions where entrainment occurred that were biased high compared with the particle-tracking model.

Introduction

Power plants, factories, and industrial facilities in the United States withdraw more than 279×10^9 gallons of cooling water a day from surface waters (U.S. Environmental Protection Agency [U.S. EPA] 2002). The withdrawal of such large quantities of water caused the U.S. Environmental Protection Agency to be concerned that substantial numbers of aquatic organisms are being adversely affected because of entrainment. Entrainment occurs when aquatic organisms, including fish eggs and newly hatched fish (ichthyoplankton), are drawn into cooling systems along with cooling water. Entrained organisms are exposed to mechanical, thermal, and sometimes, toxic stress. These stresses can cause high mortality rates for some species of entrained ichthyoplankton (U.S. EPA 2002).

The Empirical Transport Model (ETM) has been widely adopted by electric utilities and regulatory agencies for estimating the effects of entrainment mortality on fish populations in estuaries, notably the Hudson River (Electric Power Research Institute 1999). It requires data on the distribution of ichthyoplankton in the source water body and the volume of cooling water withdrawn from each region of that water body. A major assumption of the ETM is that the fraction of ichthyoplankton entrained varies only in response to changes in water withdrawals, not to changes in freshwater flow. Because freshwater flow varies in estuaries seasonally and annually, accounting for freshwater flow would make the ETM more realistic and potentially improve the accuracy of its results.

Freshwater flow can be accounted for by using a particle-tracking model to estimate region-specific entrainment probabilities. This approach would produce time-varying estimates of the fraction of ichthyoplankton, in each region, that are entrained and estimates of the number of times each

* Corresponding author; tele: 201/216-5289; e-mail: ablumber@stevens.edu

© 2004 Estuarine Research Federation

particle is entrained during a week. Estimates of the number of times ichthyoplankton are entrained can be used to refine estimates of the probability of dying because ichthyoplankton that are entrained multiple times are more likely to die than ichthyoplankton that are entrained once (Electric Power Research Institute 2000).

During 1996, the New York State Department of Environmental Conservation, environmental advocacy groups, and electric utilities were negotiating conditions of the State Pollutant Discharge Elimination System permits for power plants operating along the Hudson River. These groups jointly decided that a study should be conducted to calculate entrainment probabilities for power plants at five sites on the Hudson River using a particle-tracking model calibrated during low and high freshwater flow periods and to compare those estimates with entrainment probabilities from the ETM. The study was conducted as part of the permitting process. The methods and results are presented in this paper.

Methods

Study Location

The Hudson River estuary extends from km 0 at the southern end of Manhattan to km 247 at the Federal Dam in Troy, New York (Fig. 1). It is essentially a flooded valley with little gradient and has a mean depth ranging from 4 to 22 m. Between km 247 and km 0, the river only drops about 1.5 m, an average of 1.6 cm km^{-1}. Tides are the dominant source of water movement, reversing the direction of flow in the river twice each day. The maximum tidal excursion is about 21 km. The mean ebb current velocity is 0.4 m s^{-1} and the mean tidal flood current velocity is 0.36 m s^{-1} (Cooper et al. 1988).

The study area extended from km 33 to km 247. The power plants (Bowline Point, Danskammer, Lovett, Roseton, and Indian Point Units 2 and 3; Fig. 2) are located between km 60 and km 107 (Hutchison 1988). They can withdraw water from the river for once-through cooling at a maximum rate of 6.1×10^9 gallons per day (Central Hudson Gas and Electric Corporation et al. unpublished data). The entrainment of ichthyoplankton caused by those water withdrawals has been of considerable interest to electric utilities, the public, and regulators (Dunning et al. 2000).

Circulation Model

We used the Estuarine and Coastal Ocean Model (ECOM), a three-dimensional, time-dependent, estuarine and coastal circulation model originally developed by Blumberg and Mellor (1987) to simulate the movement of neutrally buoyant, passive particles. ECOM incorporates the Mellor-Yamada 2.5 level turbulent closure model (Mellor and Yamada 1982; Mellor 2001) that provides a realistic parameterization of vertical mixing processes. A system of curvilinear coordinates is used in the horizontal direction, allowing for a smooth and accurate representation of variable shoreline geometry. In the vertical direction, the model uses a σ-coordinate system to permit better representation of bottom topography. Water surface elevation, water velocity (in three dimensions), temperature, salinity, and water turbulence are calculated in response to meteorological conditions, freshwater inflows, tides, and temperature and salinity at the open boundaries. The model solves a coupled system of differential, prognostic equations describing the conservation of mass, momentum, temperature, salinity, turbulent energy, and turbulence on a macroscale. It has most recently been used to simulate the dynamics of St. Andrew Bay, Florida (Blumberg and Kim 2000) and New York-New Jersey estuary (Blumberg et al. 1999).

The ECOM for the Hudson River estuary has a high-resolution grid for resolving detailed hydrodynamic features between km 33 and km 118 (Fig. 1). In this region, the grid typically has 10 boxes in the cross-river plane and 10 in the vertical plane. These boxes are 200 m wide and 650 m long on average and have a minimum width of about 50 m and a minimum length of about 200 m. A lower resolution grid is used between km 118 and km 247. In this region, the grid has 3 boxes in the cross-river plane. These boxes are 300 m wide and 3,000 m long on average. A computational time step of 10 s was required to accommodate this grid system. The circulation dynamics of the ECOM are driven by surface wind stress, surface heat flux, freshwater inflows, water levels, temperature, and salinity. The influence of each power plant was simulated by specifying the rate of cooling water flow and the temperature difference between the intakes and outfalls. Cooling water was withdrawn from the grid box next to each power plant at depths corresponding to those of the intake (Fig. 2). The discharge flow was also added to the grid box next to each plant. This approach did not simulate the physical dynamics in the near-field region of the intakes and outfalls. Parameterization of the horizontal and vertical mixing processes in ECOM, together with a sufficiently refined model grid like the one used here, simulates the near-field entrainment processes sufficiently well to provide confidence that the far field results are not biased (Blumberg et al. 1996).

Particle-tracking Model

The movement of particles in the model was determined by exploiting the equivalency between

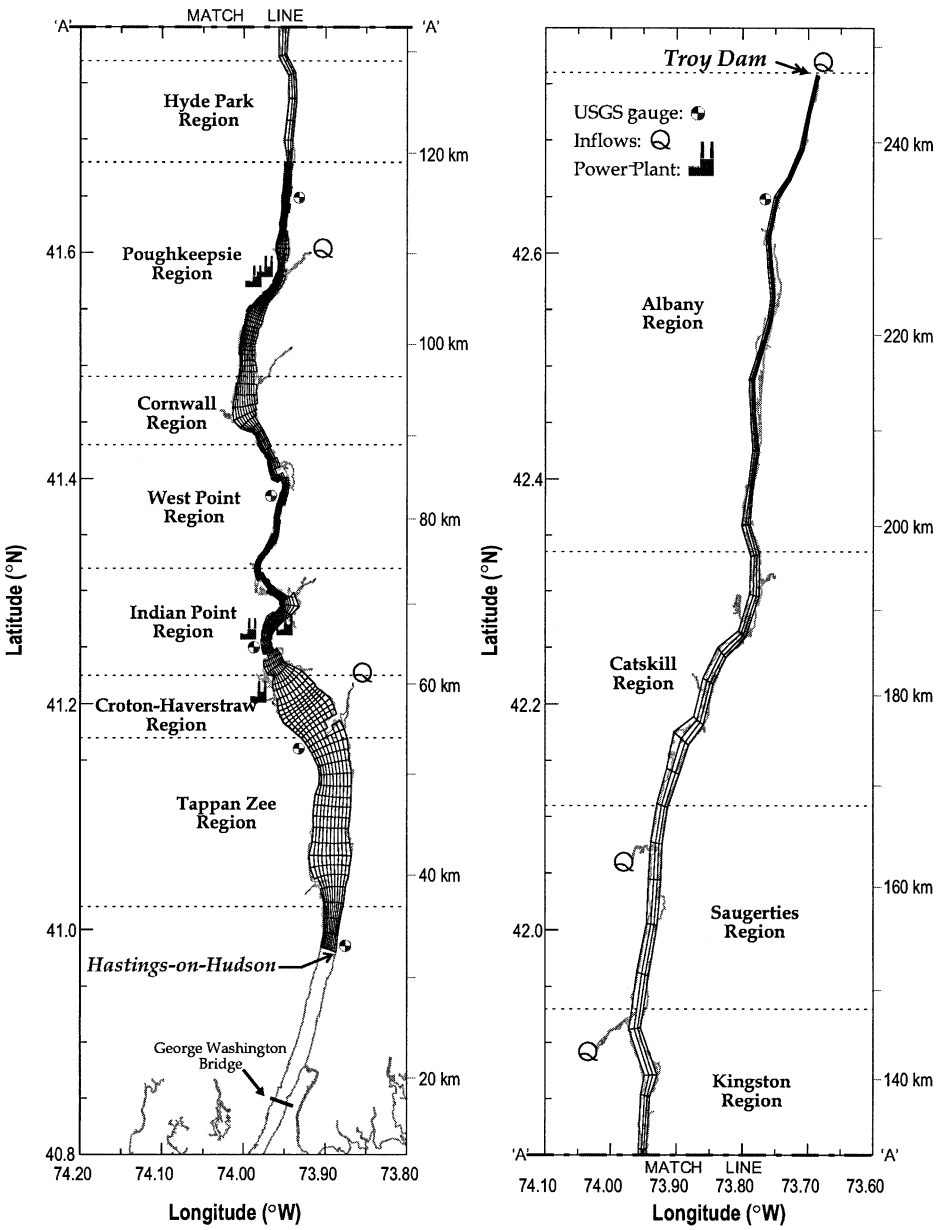

Fig. 1. Location of United States Geological Survey (USGS) gauges for measuring water level, USGS flow stations, and Hudson River power plants on the Hudson River.

tracking particles and solving a mass transport equation for a conservative substance (Tompson and Gelhar 1990). Following Dimou and Adams (1993), a random-walk, particle-tracking scheme was designed that calculated the displacement of particles as the sum of an advective component and an independent, random Markovian component that statistically approximates the dispersion characteristics of the environment. By relating the advective and Markovian components to the appropriate terms in a mass conservation equation, the distribution of particles was the same as that concentration resulting from the solution of the conservation equation.

In a three-dimensional environment, a conservative substance is transported by advection and dispersion. The solution for this transport problem is commonly based on the mass balance equation. By introducing the σ transformation in the vertical,

$$\sigma = \frac{z - \eta}{H + \eta} = \frac{z - \eta}{D} \tag{1}$$

where z is the vertical coordinate, H(x,y) is the water depth, η(x,y) is the surface elevation, and D is

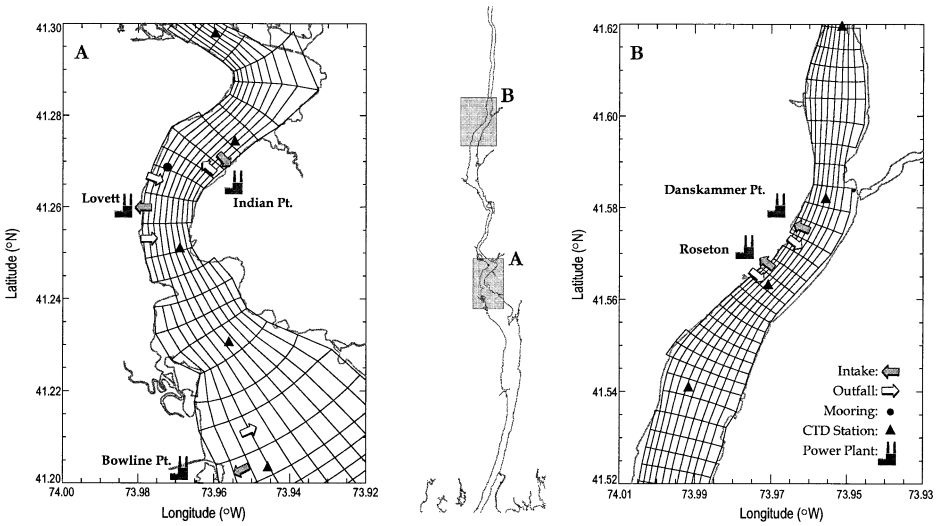

Fig. 2. Location of the power plant intakes and outfalls, and mooring stations, in relation to grid cells of the Estuarine and Coastal Ocean Model.

the total depth, H + η, the transport equation for a conservative tracer in an orthogonal curvilinear coordinate system (ξ_1, ξ_2, σ) can be written as (Blumberg and Mellor 1987):

$$h_1 h_2 \frac{\partial (DC)}{\partial t} + \frac{\partial}{\partial \xi_1}(h_2 U_1 DC) + \frac{\partial}{\partial \xi_2}(h_1 U_2 DC) + h_1 h_2 \frac{\partial (\omega C)}{\partial \sigma} = \frac{\partial}{\partial \xi_1}\left(\frac{h_2}{h_1} A_H D \frac{\partial C}{\partial \xi_1}\right) + \frac{\partial}{\partial \xi_2}\left(\frac{h_1}{h_2} A_H D \frac{\partial C}{\partial \xi_2}\right) + \frac{h_1 h_2}{D}\frac{\partial}{\partial \sigma}\left(K_H \frac{\partial C}{\partial \sigma}\right) \quad (2)$$

where

$$\omega = W - \frac{1}{h_1 h_2}\left[h_2 U_1\left(\sigma \frac{\partial D}{\partial \xi_1} + \frac{\partial \eta}{\partial \xi_1}\right) + h_1 U_2\left(\sigma \frac{\partial D}{\partial \xi_2} + \frac{\partial \eta}{\partial \xi_2}\right)\right] - \left(\sigma \frac{\partial D}{\partial t} + \frac{\partial \eta}{\partial t}\right) \quad (3)$$

t is time, C is the concentration, h_1 and h_2 are the metrics of the unit grid box in the ξ_1 and ξ_2 directions, U_1 and U_2 are the velocity components along the ξ_1 and ξ_2 directions, W is the vertical velocity (z direction), and A_H and K_H are the horizontal and vertical mixing coefficients, respectively. All are part of ECOM's set of equations. By adding

$$\frac{\partial}{\partial \xi_1}\left[\frac{\partial}{\partial \xi_1}\left(\frac{A_H}{h_1^2} h_1 h_2 D\right) C\right] + \frac{\partial}{\partial \xi_2}\left[\frac{\partial}{\partial \xi_2}\left(\frac{A_H}{h_2^2} h_1 h_2 D\right) C\right] + \frac{\partial}{\partial \sigma}\left[\frac{\partial}{\partial \sigma}\left(\frac{K_H}{D^2} h_1 h_2 D\right) C\right] \quad (4)$$

to both sides of Eq. 2 and rearranging it, the transport equation becomes

$$\frac{\partial}{\partial t}(h_1 h_2 DC) + \frac{\partial}{\partial \xi_1}\left\{\left[\frac{U_1}{h_1} + \frac{1}{h_1 h_2 D}\frac{\partial}{\partial \xi_1}\left(\frac{A_H}{h_1^2} h_1 h_2 D\right)\right] \times h_1 h_2 DC\right\} + \frac{\partial}{\partial \xi_2}\left\{\left[\frac{U_2}{h_2} + \frac{1}{h_1 h_2 D}\frac{\partial}{\partial \xi_2}\left(\frac{A_H}{h_2^2} h_1 h_2 D\right)\right] h_1 h_2 DC\right\} + \frac{\partial}{\partial \sigma}\left\{\left[\frac{\omega}{D} + \frac{1}{h_1 h_2 D}\frac{\partial}{\partial \sigma}\left(\frac{K_H}{D^2} h_1 h_2 D\right)\right] h_1 h_2 DC\right\} = \frac{\partial^2}{\partial \xi_1^2}\left(\frac{A_H}{h_1^2} h_1 h_2 DC\right) + \frac{\partial^2}{\partial \xi_2^2}\left(\frac{A_H}{h_2^2} h_1 h_2 DC\right) + \frac{\partial^2}{\partial \sigma^2}\left(\frac{K_H}{D^2} h_1 h_2 DC\right). \quad (5)$$

Equation 5 was the key link to the particle-tracking model. The starting point for the Lagrangian model was the three dimensional Langevin equation (Coffey et al. 2003):

$$\frac{\overrightarrow{dX}}{dt} = A(\vec{X}, t) + B(\vec{X}, t) Z(t) \quad (6)$$

where $\vec{X}(t)$, $A(\vec{X}, t)$ and $B(\vec{X}, t)$ are vectors, $\vec{X}(t)$ defines the position in three dimensions of a particle, $A(\vec{X}, t)$ is the deterministic particle advection, $B(\vec{X}, t)$ represents a random component that leads to particle diffusion (Solomon et al. 1994), and

Z(t) is a vector of independent random numbers with zero mean and unit variance.

If $f = f(\vec{X}, t|\vec{X}_0, t_0)$ were defined as the conditional probability density function for the positions $\vec{X}(t)$ of particles whose initial position at t_0 is $\vec{X}_0$, it would satisfy the Fokker-Planck equation (Tompson and Gelhar 1990; Brickman and Smith 2002) in the limit as the number of particles gets very large and the time step used to solve the conservation equation gets very small. The evolution of f is described as

$$\frac{\partial f}{\partial t} + \frac{\partial}{\partial \vec{X}}(Af) = \nabla^2\left(\frac{1}{2}BB^T f\right) \tag{7}$$

The transport Eq. 5 is equivalent to the Fokker-Planck Eq. 7 written in orthogonal curvilinear coordinates if $f \equiv h_1 h_2 DC$ (Thomson 1987). This Eulerian consistency relationship then provides the A function

$$\mathrm{A} \equiv \begin{bmatrix} \dfrac{U_1}{h_1} + \dfrac{1}{h_1 h_2 D}\dfrac{\partial}{\partial \xi_1}\left(\dfrac{A_H}{h_1^2} h_1 h_2 D\right) \\ \dfrac{U_2}{h_2} + \dfrac{1}{h_1 h_2 D}\dfrac{\partial}{\partial \xi_2}\left(\dfrac{A_H}{h_2^2} h_1 h_2 D\right) \\ \dfrac{\omega}{D} + \dfrac{1}{h_1 h_2 D}\dfrac{\partial}{\partial \sigma}\left(\dfrac{K_H}{D^2} h_1 h_2 D\right) \end{bmatrix} \tag{8}$$

and a relationship that yields the B function

$$\frac{1}{2}BB^T \equiv \begin{pmatrix} \dfrac{A_H}{h_1^2} & 0 & 0 \\ 0 & \dfrac{A_H}{h_2^2} & 0 \\ 0 & 0 & \dfrac{K_H}{D^2} \end{pmatrix} \tag{9}$$

$A(\vec{X}, t)$, $B(\vec{X}, t)$ in Eq. 6 were determined and the position $\vec{X}(t)$ of each particle was calculated. The development of this particle-tracking model in orthogonal curvilinear coordinates has not previously been reported in the literature.

The numerical algorithm used in the solution of Eq. 6 was based on the same orthogonal curvilinear grid structure and interpolation schemes built into ECOM. To ensure that the particle-tracking method was correct, tests comparing the method with analytical solutions were conducted (Zhang 1995). The tests involved long straight channels with flat and sloping bottoms and circular channels with open and closed lateral boundaries. The method was able to obtain the correct answer for all of these test cases.

Entrainment Probabilities

The particle-tracking simulation involved releasing neutrally buoyant, passive particles throughout the model grid at different times. The probability that a particle would be entrained at a power plant intake was expected to depend on transport from the point of release to the grid box from which water was withdrawn from the Hudson River, the amount of time spent in the grid box of the intake, and the probability of entering the intake when in the grid box.

In the Hudson River, particles are transported by tidal currents and dispersed both vertically and horizontally by turbulent diffusion. Although the net movement of water is downriver, the ebb and flow of tidal currents can transport particles to the grid box of an intake multiple times. In the model, the location of every particle was recorded at each 10-s time step. As a result, the number of particles that spend k time steps in the grid box of an intake, N_k, can be counted. The probability that a particle would be located in the grid box of an intake for k time steps is

$$P_{gb}(k) = \frac{N_k}{N} \tag{10}$$

where N is the total number of particles released from a given location. This definition of P_{gb} implicitly uses the volume of the grid box since the number of particles is counted regardless of the volume of the box itself. Physically, the volume of the box should not play a role in the analysis.

Near a power plant intake, flows are typically complex, having high swirl levels and free surface vortices, due to the layout of the intake pumps and their relatively large size (Melville et al. 1994). Although the factors causing these complex flows are well known, there is no theoretical method for predicting this nearfield behavior (Constantinescu and Patel 1998). Consequently there is no general method for determining the near-field probability of entrainment for a particle in the grid box of an intake. We expressed that nearfield probability as

$$P_{nf} = \frac{Q_{\text{plant}} \cdot \Delta T}{V} \tag{11}$$

where Q_{plant} is the volume of water withdrawn per unit time at the power plant intake and where V is the volume of the model intake grid box. Equation 11 is the ratio of the volume of water withdrawn from the intake grid box in time ΔT (i.e., one time step of 10 s) to the volume of the grid box itself. Equation 11 seems to suggest, similar to Eq. 10, that the volume of the grid box has a role in the analysis. The use of the box volume in Eq. 11 will be countered by the implicit use of volume in Eq.

10 later in the analysis. For each time step that a particle spends in the grid box of the intake, it has a probability equal to P_{nf} of being entrained. A particle that spends a total of k time steps in the grid box of the intake could be entrained and then re-entrained multiple times. Assuming that the probability of entrainment is independent for each time step that a particle spends in the grid box of the intake, then the probability that the particle would be entrained n times during the k time steps in the grid box of the intake is given by the binomial distribution

$$P_{\text{intake}}(n|k) = \binom{k}{n} P_{nf}^{n}(1 - P_{nf})^{k-n} \tag{12}$$

where

$$\binom{k}{n} = \frac{k!}{n!(k - n)!} \tag{13}$$

The joint probability that a particle would spend k time steps in the grid box of the intake and be entrained n times is the product of Eq. 10 and 12

$$P(k, n) = P_{gb}(k) \times P_{\text{intake}}(n|k) \tag{14}$$

The marginal probability that a particle released from a given location would be entrained n times, $P(n)$, is the sum of the joint probability in Eq. 14 over all values of k,

$$P(n) = \sum_{k=0}^{\infty} P(k, n) \tag{15}$$

P(0) is the probability that a particle would not be entrained. The probability that a particle would be entrained once, i.e., initial entrainment, is $P(1)$; re-entrained once, i.e., entrained twice, is $P(2)$; and so forth. The combination of P_{gb} and P_{intake} in Eq. 14 eliminates the seemingly inappropriate use of volume in each of them because P_{gb} has volume in its numerator while P_{intake} has volume in its denominator.

Prior to estimating the entrainment probabilities, a sensitivity run was conducted to determine if the number of released particles, their time of release within a tidal cycle, or their initial lateral position within a cross section would effect the probability of entrainment. The presence of relatively complex tidal currents in the Hudson River created a dynamic environment where particles released on the ebb portion of the tidal cycle followed very different trajectories from those released on flood cycle. The lateral shear in current field also played a role in the path of released particles. The distribution of particles released along the banks of the river tended to be streaky and patch-like because currents there were slow, an order of magnitude slower than those in the middle of the river. These findings are in agreement with what is known about dispersion in tidally dominated waters (Geyer and Signell 1992). The errors associated with underseeding of particles were more difficult to quantify. Experiments where the number of released particles was varied were not definitive. There are relatively few studies of particle trajectory calculations in estuarine systems and none provide real insight into the number of particles required (Garvine et al. 1997). We used as many particles as computationally feasible, which was more than the number in previous studies (Brown et al. 2000).

To obtain stable probability statistics, 100 particles were released every hour from 11 different regions. The 11 regions correspond to segments of the Hudson River used in entrainment studies (Fig. 1). An array of 25 horizontal and 4 vertical release positions were used for the 6 wider regions (Tappan Zee, Croton-Haverstraw, Indian Point, West Point, Cornwall, and Poughkeepsie) and an array of 10 horizontal and 10 vertical release positions were used in the 5 narrower regions (Hyde Park, Kingston, Saugerties, Catskill, and Albany), so 1,100 particles were released every hour and their positions recorded every 10 s, the model time step. The low flow release period began August 9, 1997 and the high flow period began on March 19, 1998.

Particles were released hourly for 7 d and then tracked for the following 7 d. Almost 185,000 particles were used in the analysis. The 7-d time period was selected because ichthyoplankton sampling in the Hudson River has historically occurred weekly providing for an opportunity to validate this Lagrangian approach against that data in a future study. To estimate the probabilities of entrainment and re-entrainment, the cumulative time various numbers of particles spent in a particular intake box was calculated for releases from all of the regions.

Data Collection

Coastal Oceanographic Associates collected data on currents, temperature, and salinity in the Hudson River during low and high freshwater flow conditions and we obtained data on water levels, freshwater inflows, temperature, salinity, and meteorology from the U.S. Geological Survey (USGS) and the National Oceanic and Atmospheric Administration (USGS 1998; Lott et al. 2001). The period of low freshwater flow was August 14–30, 1997, and the period of high freshwater flow was March 25–April 9, 1998. Relatively high ichthyoplankton abundance historically occurs during the periods of both the low and high freshwater flow (Central

Hudson Gas and Electric Corporation et al. unpublished data).

A series of 8 shipboard velocity surveys and 2 large-scale hydrographic surveys were conducted during the periods of high freshwater flow; half during the spring tidal phase and half during the neap tidal phase (Dragos and Geyer 1998a). A series of 4 shipboard velocity surveys and a large-scale hydrographic survey were conducted during the period of low freshwater flow (Dragos and Geyer 1998b). The velocity surveys, extending from km 53 to km 108, consisted of measurements during 12-h surveys using an acoustic Doppler current profiler (ADCP). Vertical profiles of temperature and salinity along the channel of the river were taken at discrete stations during the ADCP surveys. A mooring was deployed at km 67 concurrent with the shipboard measurements to record currents, bottom pressure, temperature, and salinity over each entire study period.

Hourly data on water elevations from gauges at Albany (km 234), Poughkeepsie (km 115), West Point (km 82), Tomkins Cove (km 64), Congers (km 53), and Hastings-on-Hudson (km 33) were obtained from USGS as were daily data at the Troy Dam (km 247), Esopus Creek (km 164), Rondout Creek (km 146), Wappinger Creek (km 107), and Croton River (km 53). The Hudson River discharge at Troy is by far the largest source of flow. During the low-flow period, the discharge was a fairly constant 125 $m^3 s^{-1}$. During the high-flow period more variability was observed. The discharge in the early part of the period was 750 $m^3 s^{-1}$ and increased to 2,400 by the end of the 30 d. It averaged 1,200 $m^3 s^{-1}$.

The two major surface forcing functions, surface heat flux and wind stress, were computed from the 3-h air temperature, air pressure, relative humidity, cloud coverage, wind speed, and wind direction data from Albany, New York, and Central Park, New York City. Daily temperatures at the intake and outfall of each of the five power plants and daily flows at the intake were obtained from records at the power plants for the periods of low and high freshwater flow (Table 1).

The hydrodynamic model was run for two 30-d flow periods: August 1–30, 1997, and March 11–April 9, 1998. It was calibrated and validated using data collected in the Hudson River from August 14–30, 1997, and March 25–April 9, 1998. The first 2 d of each 30-d flow period were considered spin-up of the model and ignored. The specific mathematical formulation for the model boundary conditions were the same as those used by Blumberg et al. (1999). The horizontal viscosities and diffusivities were based on the formulation of Smagorinsky (1963) with its associated constant found here to be 0.1. This produced values of about 10 $m^2 s^{-1}$ for these horizontal mixing coefficients. The vertical mixing coefficients were about 50 $cm^2 s^{-1}$ when the water column is well mixed and about 5 $cm^2 s^{-1}$ when it is stratified. A quadratic bottom friction was used with the bottom frictional drag coefficient $C_d = 1.5 \times 10^{-3}$.

ETM Calculations

The conditional morality rate (CMR) for entrainment computed using the ETM is a weighted average of cohort-specific and region-specific estimates of conditional survival rates calculated as:

$$\hat{CMR} = 1 - \sum_c \rho_c \left\{ \prod_t \left[1 - \sum_k D_{k,t,c} PE_{k,t,c} PDE_{t,c} \right]^{\delta_{t,c}} \right\} \quad (16)$$

where $\hat{CMR}$ is the estimate of CMR, ρ_c is the proportion of the total annual spawn due to weekly cohort c, $D_{k,t,c}$ is the proportion of weekly cohort c that inhabits river region k during calendar week t, $PE_{k,t,c}$ is the probability of entrainment for calendar week t for fish of cohort c who begin the week in river region k, $PDE_{t,c}$ is the probability that a fish of cohort c, that becomes entrained during calendar week t, dies from being entrained, and $\delta_{t,c}$ is a binary variable that has a value of 1 if fish of

TABLE 1. The average, maximum, and minimum cooling water flow and temperature difference between the intake and discharge (ΔT) of the Indian Point, Lovett, Bowline Point, Roseton, and Danskammer power plants for periods of high freshwater flow (March 25–April 9, 1998) and low freshwater flow (August 14–30, 1997) in the Hudson River.

	Cooling Water Flow ($m^3 s^{-1}$)						ΔT (°C)					
	Low Flow			High Flow			Low Flow			High Flow		
Power Plant	Average	Maximum	Minimum	Average	Maximum	Minimum	Average	Maximum	Minimum	Average	Maximum	Minimum
Indian Point	76	111	54	42	48	38	6	10	0	10	12	7
Lovett	12	17	7	7	10	2	8	10	6	8	12	4
Bowline Point	21	39	5	20	40	4	4	6	0	2	4	0
Roseton	24	40	1	25	26	20	3	9	0	5	9	0
Danskammer	16	18	13	9	9	8	7	9	6	12	14	7

cohort c are in an entrainable life stage during week t and a value of 0 otherwise; and

$$PE_{k,t,c} = 1 - \exp - \left(\frac{Q_t f_k}{V_k} W_{t,c} \right) \qquad (17)$$

where Q_t is the volume of water withdrawn by the power plant during week t, f_k is the fraction of water withdrawn from the power plant that originates in river region k, V_k is the volume of river region k, and $W_{t,c}$ is the ratio of the average density of fish (i.e., number m^{-3}), from cohort c during calendar week t, in the river region adjacent to the power plant intake to the density of those fish within the power plant intake.

The term within the outer brackets of Eq. 16 is the lifetime conditional survival rate for cohort c. The overall CMR estimate for the population of fish is the weighted average of these cohort-specific estimates of CMR, where the parameters ρ_c are the weighting factors.

The term within the inner brackets of Eq. 16 is a conditional survival rate: the probability that a fish of cohort c does not die from entrainment (by either not being entrained or by surviving entrainment if it is entrained) during calendar week t, given no other forces of mortality act on the fish during the week. This term is the complement of the weighted average of cohort-specific and region-specific estimates of conditional mortality rates, where the parameters $D_{k,t,c}$ are the weighting factors.

To compare estimates of entrainment probability from the particle-tracking model to corresponding estimates from the ETM, we calculated estimates of the probability of entrainment for the ETM using Eq. 17 and values of $W_{t,c}$ and f_k from Central Hudson Gas and Electric Corporation et al. (unpublished data). The value of $W_{t,c}$ was always 1.0. The value of f_k was assumed to be proportionate to the fraction of the volume of the river region that was withdrawn as cooling water. The rate of water withdrawal from each river region was assumed to be a constant fraction of the total water withdrawn for cooling water by a power plant. The total withdrawal volume among regions was apportioned based on the size of the regions and distance of tidal transport over one tidal cycle, which was assumed to be 6.5 miles in each direction under all flow conditions and in all regions.

Results

Model Predictions

The salinities, water temperatures, current velocities, and water surface elevations predicted by the model closely corresponded to the data collected in the Hudson River. We present results from the period of low freshwater flow because the hydrodynamics during this period were complicated by the presence of saltwater in the study area as far upriver as km 70. Saltwater was not present in the study area during the period of high freshwater flow.

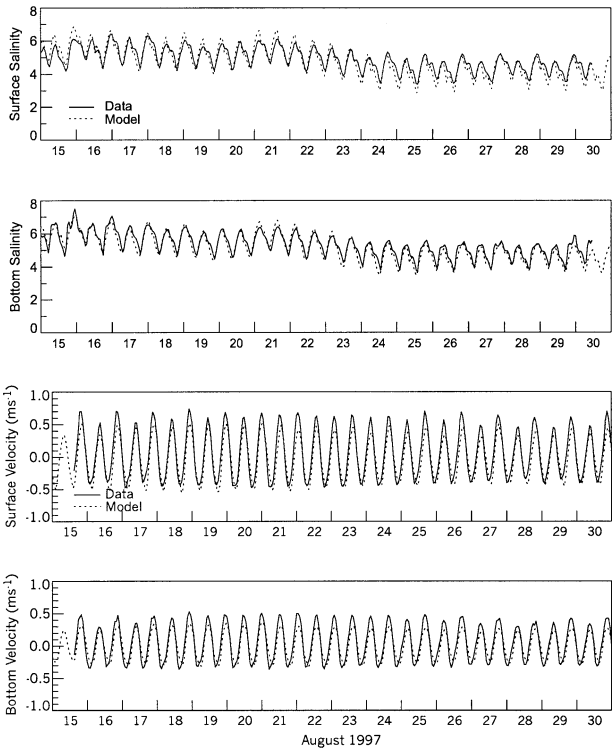

Fig. 3. Surface and bottom salinity and current velocities from data collected in the Hudson River and predicted by the Estuarine and Coastal Ocean Model in August 1997 at a mooring station near the Indian Point power plant.

The temporal patterns of salinity and current velocity predicted by the model in the surface and bottom layers and those measured in the river had similar low frequency variability and properly phased tidal oscillations during the 15 d of low flow when data were collected at the km 67 mooring station (Fig. 3). The 15-d average salinities predicted by the model and those measured in the river differed by only 0.2 psu at the surface (4.9–4.7 psu) and 0.3 psu on the bottom (5.4–5.1 psu).

The locations of isohalines predicted by the model and their shape at the end of the low-flow period were similar to those based on data collected in the river (Fig. 4) notwithstanding considerable changes in the salinity pattern during the low-flow period. Although salinity and current velocity were variable, water temperature at the km-67 mooring station was relatively constant, varying from only 24.5°C to 27.0°C. The 15-d average temperatures predicted by the model and those mea-

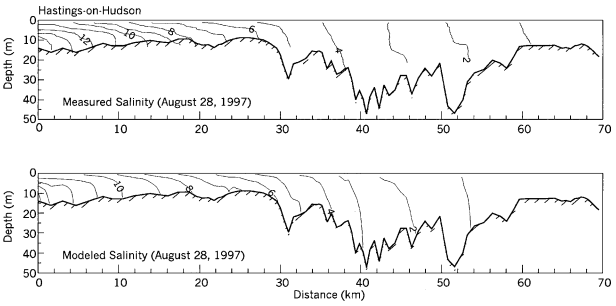

Fig. 4. Isohalines between km 0 and km 70 from data collected in the Hudson River and predicted by the Estuarine and Coastal Ocean Model.

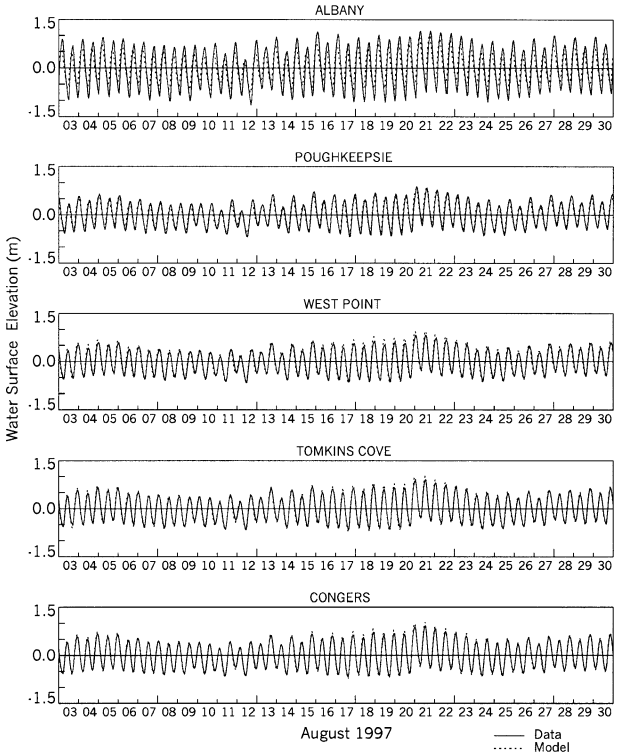

Fig. 5. Water surface elevations from United States Geological Survey gauges at Congers, Tompkins Cove, West Point, Poughkeepsie, and Albany in August 1997.

sured in the river differed by only 0.2°C at the surface and 0.3°C on the bottom.

The temporal pattern of water surface elevation predicted by the model within the area of the high-resolution grid (km 33 to km 118) and those at 3 gauges in that area were in good agreement. They had similar low frequency variability and properly phased tidal oscillations during the 28-d simulation (Fig. 5). The amplitude and phase differences between the data and the model increased from downstream to upstream. At km 234 both amplitude error and phase error were relatively large (about 35% and 30%, respectively), the result of an overly coarse model grid in the northern portions of the study area.

Entrainment Probabilities

Particle-tracking Model

Based on the particle-tracking model, the cumulative time that particles released in a river region with a power plant spent in the grid box next to the power plant intake over a 1-wk period differed depending on the plant's nearfield entrainment probability (Table 2) and on freshwater flow in the Hudson River. Most of the particles released in the Indian Point region during the low-flow period spent less than 20 min in the grid box next to the Indian Point intakes; far fewer spent more than 90 min there (Fig. 6). During the high-flow period, the pattern was similar to that during the low-flow period except that no particles spent more than 90 min in the grid box next to the Indian Point intakes. A similar difference between the low-flow and high-flow periods occurred for particles released in river regions where the other power plants were located.

During the low-flow period, the number of river regions with a probability of initial entrainment greater than zero ranged from 4 at Roseton to 6 at Indian Point, Lovett, and Bowline. The probability of initial entrainment peaked for particles released in the same river region as a power plant except at Bowline, where the peak probability of

TABLE 2. The near field probability of entrainment for a particle spending one time step in the grid box for the intakes of the Indian Point, Lovett, Bowline Point, Roseton, and Danskammer power plants during low-flow and high-flow periods and the volume of the grid box for each intake.

		Near-field Entrainment Probability (10^{-3}%)					
	Volume of Intake Cell	Low Flow			High Flow		
Power Plant	(10^5 m^3)	Average	Maximum	Minimum	Average	Maximum	Minimum
Indian Point	7.96	10	14	7	5	6	5
Lovett	5.43	2	3	1	1	2	<1
Bowline Point	21.70	1	2	<1	1	2	<1
Roseton	3.21	8	13	<1	8	8	6
Danskammer	8.06	2	2	2	1	1	1

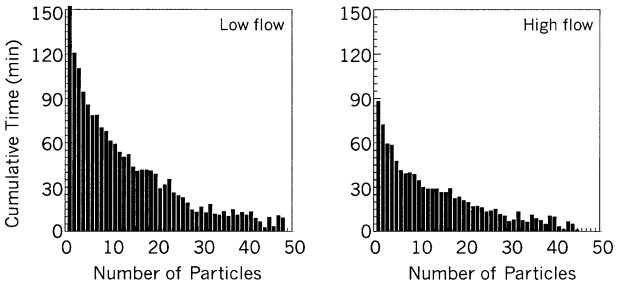

Fig. 6. Cumulative time particles spent in the grid box for the Indian Point intake during the low-flow period and high-flow period. Particles were released in the Indian Point region and tracked for 7 d.

initial entrainment was slightly higher in the river region just upriver of the power plant than in the region of the power plant (Table 3). Both the peak probability of initial entrainment and the average across all regions were highest at Indian Point, the power plant with the highest cooling water intake flows (Table 1). The probability of re-entrainment once was low relative to initial entrainment; less than 1% at all of the power plants except Indian Point where it was 1.5% for particles released in the Indian Point region and 1% for particles released in the West Point region. The probability of re-entrainment twice was less than 0.2% at all of the power plants.

During the high-flow period, the number of river regions with a probability of initial entrainment greater than zero ranged from 6 at Danskammer and Roseton to 9 at Indian Point, Lovett, and Bowline; nearly all were upriver of the power plants. Both the peak probability of initial entrainment and the average across all regions were lower than during the low-flow period except that the average for Bowline was higher (Table 4). The peak probability of initial entrainment was highest for particles released in the river region upriver of each power plant except for Bowline, where it was nearly so. The probability of re-entrainment once was low relative to initial entrainment; less than 0.2% at all of the power plants.

ETM

Based on the ETM, the number of river regions with a probability of initial entrainment greater than zero during the low-flow period ranged from 2 at Danskammer and Roseton to 3 at Indian Point, Lovett, and Bowline (Table 3). The probability of initial entrainment peaked for particles released in the same river region as a power plant.

During the high-flow period, the number of river regions with a probability of initial entrainment greater than zero ranged from 2 at Danskammer to 3 at Indian Point, Roseton, Lovett, and Bowline (Table 4). The probability of initial entrainment peaked for particles released in the same river region as a power plant and was lower than that during the low-flow period except at Roseton where it was slightly higher.

Discussion

The profound effect of freshwater flow on the probability of entrainment was evident from results of the particle-tracking model. Both the number of river regions from which particles were entrained and the probabilities of entrainment for particles in those river regions differed between the low-flow and high-flow periods. During the high-flow period, particles spent less time in the grid box next to the intakes, reducing the probability of entrainment for particles released in the river region of each power plant and the average probability of entrainment across all regions at In-

TABLE 3. Probability that a particle would be entrained one time at the intake of the Danskammer, Roseton, Indian Point, Lovett, and Bowline power plants if the particle were released in the same river region as the power plant during the low-flow period estimated with the particle-tracking model (PTM) and the Empirical Transport Model (ETM). Underlined numbers indicate the location of the power plant in the column heading.

	Probability of Entrainment (%)									
	Danskammer		Roseton		Indian Point		Lovett		Bowline	
River Region	PTM	ETM	PTM	ETM	PTM	ETM	PTM	ETM	PTM	ETM
Albany	0.000	0.000	0.000	0.000	0.000	0.000	0.000	0.000	0.000	0.000
Catskill	0.000	0.000	0.000	0.000	0.000	0.000	0.000	0.000	0.000	0.000
Saugerties	0.001	0.000	0.000	0.000	0.000	0.000	0.000	0.000	0.000	0.000
Kingston	0.069	0.000	0.035	0.000	0.000	0.000	0.000	0.000	0.000	0.000
Hyde Park	0.594	0.000	0.438	0.000	0.000	0.000	0.000	0.000	0.000	0.000
Poughkeepsie	1.577	2.100	2.141	3.480	0.197	0.000	0.027	0.000	0.007	0.000
Cornwall	0.012	1.350	0.020	2.790	2.386	0.000	0.362	0.000	0.134	0.000
West Point	0.000	0.000	0.000	0.000	6.935	3.050	1.243	0.290	0.635	0.000
Indian Point	0.000	0.000	0.000	0.000	9.270	11.660	2.253	1.890	1.498	2.240
Croton-Haverstraw	0.000	0.000	0.000	0.000	1.625	8.850	0.569	1.800	1.241	3.030
Tappan Zee	0.000	0.000	0.000	0.000	0.214	0.000	0.070	0.000	0.261	1.060
Average all regions	0.188	0.288	0.220	0.523	1.719	1.963	0.377	0.332	0.315	0.528

TABLE 4. Probability that a particle would be entrained one time at the intake of the Danskammer, Roseton, Indian Point, Lovett, and Bowline power plants if the particle were released in the same river region as the power plant during the high-flow period estimated with the particle-tracking model (PTM) and the Empirical Transport Model (ETM). Underlined numbers indicate the location of the power plant in the column heading.

	Probability of Entrainment (%)									
	Danskammer		Roseton		Indian Point		Lovett		Bowline	
River Region	PTM	ETM	PTM	ETM	PTM	ETM	PTM	ETM	PTM	ETM
Albany	0.048	0.000	0.096	0.000	0.000	0.000	0.000	0.000	0.000	0.000
Catskill	0.254	0.000	0.608	0.000	0.002	0.000	0.001	0.000	0.000	0.000
Saugerties	0.353	0.000	1.025	0.000	0.517	0.000	0.087	0.000	0.033	0.000
Kingston	0.384	0.000	1.104	0.000	1.912	0.000	0.391	0.000	0.406	0.000
Hyde Park	0.404	0.000	1.191	2.910	2.220	0.000	0.456	0.000	0.766	0.000
Poughkeepsie	0.219	1.460	0.774	3.620	2.137	0.000	0.474	0.000	0.963	0.000
Cornwall	0.000	0.760	0.000	2.790	2.192	0.000	0.471	0.000	0.972	0.000
West Point	0.000	0.000	0.000	0.000	2.556	1.700	0.522	0.170	0.936	0.000
Indian Point	0.000	0.000	0.000	0.000	1.882	6.620	0.434	1.100	0.970	2.130
Croton-Haverstraw	0.000	0.000	0.000	0.000	0.021	4.990	0.017	1.050	0.384	2.890
Tappan Zee	0.000	0.000	0.000	0.000	0.000	0.000	0.000	0.000	0.008	1.010
Average all regions	0.139	0.185	0.400	0.777	1.120	1.109	0.238	0.193	0.453	0.503

dian Point, Lovett, and Danskammer. The reduced probability of entrainment for particles released in the Bowline and Roseton river regions was offset by higher entrainment for particles upriver of these power plants.

Although the average probabilities of entrainment across all river regions estimated with the particle-tracking model and the ETM were relatively similar for some power plants at high flow, low flow, or both, the probabilities for each river region differed considerably between the models. The number of river regions from which particles were entrained using the ETM was consistently underestimated, resulting in probabilities for regions where entrainment occurred that were biased high compared with the particle-tracking model. At two power plants, the probability of entrainment was estimated to be greater than zero with the ETM in a river region where the probability was zero with particle-tracking model. These results are important because the fraction of all ichthyoplankton in the Hudson River that are present in each river region differs by week and year.

It appears that entrainment probabilities estimated using the particle-tracking model would provide more accurate estimates of entrainment mortality rates than those based on an assumption of the ETM that the fraction of ichthyoplankton entrained each week varies only in response to changes in water withdrawals. The probabilities of entrainment estimated for the low-flow and high-flow periods could be used to reflect the time-varying tidal and freshwater flow conditions specific to each week and river region. Interpolating between the high-flow and low-flow periods would provide the fraction of the ichthyoplankton population entrained within a river region at the level of freshwater flow that occurred during each week.

It is reasonable to ask if entrainment probabilities based on neutrally buoyant, passive particles are representative of ichthyoplankton in the Hudson River. The answer likely depends on the species, life stage, and length of the ichthyoplankton. The eggs of bay anchovy (*Anchoa mitchilli*), a species with a relatively high entrainment mortality rate at Hudson River power plants (Central Hudson Gas and Electric Corporation et al. unpublished data), are pelagic (Bigelow and Schroeder 2002) while those of Atlantic tomcod (*Microgadus tomcod*), another species with a relatively high entrainment mortality rate, are negatively buoyant. Although some larval fishes in partially mixed estuaries undergo active vertical migrations to accomplish selective tidal transport (Fortier and Leggett 1983), capelin (*Mallotus villosus*) larvae smaller than 7 mm and herring (*Clupea harengus harengus*) larvae smaller than 10 mm in the St. Lawrence estuary, were essentially passive and their dispersal was controlled by tidal processes (Fortier and Leggett 1983). If data are available indicating that eggs are not buoyant and larvae actively migrate, such behavior can be incorporated into the particle-tracking model that we used.

Acknowledgments

Funding for this study was provided by Central Hudson Gas & Electric Corp., Consolidated Edison Company of New York, Inc., New York Power Authority, and Orange and Rockland Utilities, Inc. A. F. Blumberg was also supported under Office of Naval Research grant, N00014-03-1-0633. Project guidance from William Saksen of Orange and Rockland Utilities, Inc. was most helpful. The authors are also grateful to John Young of Applied Science Associates (ASA) Analysis & Communication for his many constructive comments and suggestions and to Paul Dragos of Coastal Oceanographic Associates for providing much of the observational data.

Literature Cited

Bigelow, H. B. and W. C. Schroeder. 2002. Fishes of the Gulf of Maine, 3rd edition. Smithsonian Institution Press, Washington, D.C.

Blumberg, A. F., Z. G. Ji, and C. K. Ziegler. 1996. Modeling outfall plume behavior using far field circulation model. *Journal of Hydraulic Engineering* 122:610–616.

Blumberg, A. F., L. A. Khan, and J. P. St. John. 1999. Three-dimensional hydrodynamic model of New York Harbor region. *Journal of Hydraulic Engineering* 125:799–816.

Blumberg, A. F. and B. N. Kim. 2000. Flow balances in St. Andrew Bay revealed through hydrodynamic simulations. *Estuaries* 23:21–33.

Blumberg, A. F. and G. L. Mellor. 1987. A description of a three dimensional coastal ocean circulation model, p. 1–16. *In* N. Heaps (ed.), Three Dimensional Coastal Ocean Models, Volume 4. American Geophysical Union, Washington, D.C.

Boreman, J. and C. P. Goodyear. 1988. Estimates of entrainment mortality for striped bass and other fish species inhabiting the Hudson River estuary. *American Fisheries Society Monograph* 4:152–160.

Brickman, D. and P. C. Smith. 2002. Lagrangian stochastic modeling in coastal oceanography. *Journal of Atmospheric and Oceanic Technology* 19:83–99.

Brown, C. A., G. A. Jackson, and D. A. Brooks. 2000. Particle transport through a narrow tidal inlet due to tidal forcing and implications for larval transport. *Journal of Geophysical Research* 105:24141–24156.

Coffey, W. T., Y. P. Kalmykov, and J. T. Waldron. 2003. The Langevin Equation: With Applications to Stochastic Problems in Physics, Chemistry and Electrical Engineering, 2nd edition. World Scientific Publishing Co., Inc., River Edge, New Jersey.

Constantinescu, G. S. and V. C. Patel. 1998. Numerical model for simulation of pump-intake flow and vortices. *Journal of Hydraulic Engineering* 124:123–134.

Cooper, J. C., F. R. Cantelmo, and C. E. Newton. 1988. Overview of the Hudson River estuary. *American Fisheries Society Monograph* 4:11–24.

Dimou, K. N. and E. E. Adams. 1993. A random-walk, particle tracking model for well-mixed estuaries and coastal waters. *Estuarine, Coastal and Shelf Science* 37:99–110.

Dragos, P. and W. R. Geyer. 1998a. Entrainment of passive particles into Hudson River power plants: Data report for the low-discharge condition survey. Coastal Oceanographic Associates, Sandwich, Massachusetts.

Dragos, P. and W. R. Geyer. 1998b. Entrainment of passive particles into Hudson River power plants: Data report for the high-discharge condition survey. Coastal Oceanographic Associates, Sandwich, Massachusetts.

Dunning, D. J., Q. E. Ross, and M. W. Merkhofer. 2000. Multiattribute utility analysis for addressing Section 316(b) of the Clean Water Act. *Environmental Science and Policy* 3:S7-S14.

Electric Power Research Institute. 1999. Catalog of Assessment Methods for Evaluating the Effects of Power Plant Operations on Aquatic Communities. Electric Power Research Institute, Palo Alto, California.

Electric Power Research Institute. 2000. Review of Entrainment Survival Studies: 1970–2000. Electric Power Research Institute, Palo Alto, California.

Fortier, L. and W. C. Leggett. 1983. Vertical migrations and transport of larval fish in a partially mixed estuary. *Canadian Journal of Fisheries and Aquatic Sciences* 40:1543–1555.

Garvine, R. W., C. E. Epifanio, C. C. Epifanio, and K.-C. Wong. 1997. Transport and recruitment of blue crab larvae: A model with advection and mortality. *Estuarine, Coastal and Shelf Science* 45:99–111.

Geyer, W. R. and R. P. Signell. 1992. A reassessment of the role of tidal dispersion in estuaries and bays. *Estuaries* 15:97–108.

Hutchison, Jr., J. B. 1988. Technical descriptions of Hudson River electricity generating stations. *American Fisheries Society Monograph* 4:113–120.

Lott, N., T. Ross, and A. Graumann. 2001. NCDC products and services guide. National Climatic Data Center, Asheville, North Carolina.

Mellor, G. and T. Yamada. 1982. Development of a turbulence closure model for geophysical fluid problems. *Reviews of Geophysics and Space Physics* 20:851–875.

Mellor, G. L. 2001. One-dimensional ocean surface layer modeling: A problem and a solution. *Journal of Physical Oceanography* 31:790–809.

Melville, B. W., R. Ettema, and T. Nakato. 1994. Review of flow problems at water intake pump sumps. EPRI Research Project RP3456-01, final report. Iowa Institute of Hydraulic Research, The University of Iowa, Iowa City, Iowa.

Smagorinsky, J. 1963. General circulation experiments with the primitive equations, I. The basic experiment. *Monthly Weather Review* 91:99–164.

Solomon, T. H., E. R. Weeks, and H. L. Swinney. 1994. Chaotic advection in a two-dimension flow: Levy flights and anomalous diffusion. *Physica D: Nonlinear Phenomena* 76:70–84.

Thomson, D. J. 1987. Criteria for the selection of stochastic models of particle trajectories in turbulent flows. *Journal of Fluid Mechanics* 180:529–556.

Tompson, A. F. B. and L. W. Gelhar. 1990. Numerical simulation of solute transport in three-dimensional randomly heterogeneous porous media. *Water Resources Research* 26:2541–2562.

U.S. Environmental Protection Agency (U.S. EPA). 2002. National pollutant discharge elimination system—Proposed regulations to establish requirements for cooling water intake structures at Phase II existing facilities, proposed rule. *Federal Register* 67:17122–17225.

U.S. Geologic Survey (USGS). 1998. Water Resources Data for New York, Water Years 1997, 1998. Water Resources Division, U.S. Geological Survey, Troy, New York.

Zhang, X. Y. 1995. Ocean outfall modeling—Interfacing near and far field models with particle tracking method. Ph.D. Dissertation, MIT, Cambridge, Massachusetts.

Source of Unpublished Materials

Central Hudson Gas and Electric Corporation, Consolidated Edison Company of New York, Inc., New York Power Authority, and Southern Energy New York. Unpublished data. 1999 draft environmental impact statement for state pollutant discharge elimination system permits for Bowline Point 1 and 2, Indian Point 2 and 3, Roseton 1 and 2 steam electric generating stations. New York State Department of Environmental Conservation, Albany, New York.

Received, April 9, 2003
Revised, December 12, 2003
Accepted, December 19, 2003